Soil-Structure Interaction for Integrated Design of Weakened and Damped Structures

SOIL-STRUCTURE INTERACTION FOR INTEGRATED DESIGN OF WEAKENED AND DAMPED STRUCTURES

Gian Paolo Cimellaro[1], Diego Lopez-Garcia[2] and Andrei M. Reinhorn[3]

ABSTRACT

Previous research has shown the effectiveness of the integrated design of weakening and damping techniques (WeD) for the seismic retrofitting of structures. Indeed WeD techniques are able reducing inter-story drifts and total accelerations, the two major performance measures to evaluate the seismic behaviour of structures. Past research has been applied to fixed based structures considering relatively stiff soil conditions. It has been suspected, though, that using such techniques in soft soil sites while considering soil structure interaction, may diminish some of the advantages observed in past research. This paper examines the effect of site conditions and soil-structure interaction on the seismic performance of Weakening and Damping techniques.
An established rheological soil-shallow foundation–structure model with equivalent linear soil behaviour and nonlinear behaviour of the superstructure has been used. A large number of models incorporating wide range of soil, foundation and structural parameters were generated using robust Monte-Carlo simulation. The various structural models, along with the various site conditions, have been used for the comparative study. The design methodologies previously developed by the authors have been applied to each model considering different site conditions leading to the optimal weakening and damping. The results of the comparative study are used to quantify the effects of site conditions and foundation flexibility on the performance of the retrofitted structures.

KEYWORDS: weakening, weakening and damping, integrated design, damping, viscous, Optimization, soil structure interaction, passive control.

---

[1] Associate Professor, Department of Civil and Structural and Geotechnical Engineering, Politecnico di Torino, Corso Duca degli Abruzzi 24, 10129 Torino, Italy, E-mail: gianpaolo.cimellaro@polito.it.

[2] Department Chair, Departamento de Ingenieria Estructural y Geotecnica, Pontificia Universidad Catolica de Chile. Av. Vicuna Mackenna 4860, Macul, Santiago 782-0436, CHILE

[3] Department of Civil Structural and Environmental Engineering, University at Buffalo, 135 Ketter Hall, Buffalo, NY 14260-4300

INTRODUCTION

In the last thirty years, many researchers have been focusing on *integrated design* of structural/control systems and in *weakening and damping* techniques [1] which might be considered as a subgroup of integrated design. Integrated optimal structural/control system design has been acknowledged as an advanced design methodology for space structures, but not many applications can be found in civil engineering. Onoda and Haftka [2] minimized the weight of a structure and controller subject to constraints on the magnitude of structural responses. Salama et al. [3] realized the simultaneous design of structure and control system for a composite objective function that is a linear combination of structural and control objective functions. More recently, Curadelli and Amani [4] applied the concept of integrated design for linear structures with passive systems in the frequency domain. Similar approach has been used by Xu [5] using genetic algorithm to solve the optimization problem with discrete and continuous design variables. After the initial work by Viti et al. [6] on weakening and damping techniques different approaches have been presented such as the two stage procedure for designing *weakening and damping* techniques (WeD) [7][8] for both linear [9] and nonlinear structures [10]. Sarlis et al. [11] introduced a negative stiffness device (NSD) for buildings which can emulate *weakening* and is based on a self-contained highly compressed spring in a double negative stiffness magnification mechanism. They tested both analytically and experimentally proving the feasibility of the weakening methods.

Recently Pasala et al. [12] introduced the concept of *apparent weakening* which can be obtained by simulating yielding in an elastic system by adding a NSD, while controlling the displacements with viscous devices. Recently the same concept has also been used to

control the cable vibrations [13]. However, in none of the methods available in literature the effect of soil-structure interaction has ever been taken into account.

The paper is analyzing the effect of soil-structure interaction (SSI) on the design of WeD techniques. Different types of soil have been considered assuming a rigid, but massless surface foundation. The steady-state response of the structure is determined using the usual structural analysis methods, combined with the matrix of dynamic impedance functions which are provided in dimensionless graphical or tabular forms in the work of Gazetas [14].

SOIL-STRUCTURE INTERACTION

The assumption that a structure is fixed on the ground surface of geologic media may lead to some deviations in the analysis results of the integrated design, especially for structures on a soft base. In reality, a structure is mounted on the foundation that is in turn supported and surrounded by soil with various properties. The system analyzed in this paper is actually composed of three parts: *structure*, *foundation* and the *soil base*, which interact each other.

Interaction types

There are two kinds of interaction taking place with a vibrating structure on soil which are called:

1) kinematic interaction;
2) inertial interaction.

The *kinematic interaction* is the interaction between the soil and foundation, which causes the motion of the foundation to be different from the *displacement free field*

motion X_0. In this case, the structure above the foundation is assumed massless (Figure 1a) and the foundation motion is called *foundation input motion* (FIM). The kinematic interaction is described by a frequency dependent transfer function $S_k(\omega)$ that relates the free field motion and the FIM.

The *inertial interaction* is caused by the inertia of the structure due to its own vibration. The system is subjected to inertial forces transferred to the structure by the kinematic interaction (Figure 1b) that causes the displacements of the foundation. It can be modeled using an impedance function composed of stiffness and damping characteristics between the foundation and the soil. The global motion of the foundation is therefore the sum of these two parts

$$X = \underbrace{S_k(\omega) X_0}_{\substack{\text{kinematic} \\ \text{interaction} \\ \text{(FIM)}}} + \underbrace{X_1}_{\substack{\text{Inertial} \\ \text{interaction}}} \quad ; \tag{1}$$

where X_0 is the free field motion; $S_k(\omega)$ is the transfer function that describes the kinematic interaction and ω is the circular frequency. When the structure rests on a fixed base (infinitely stiff soil), the transfer function $S_k(\omega)$ is a unit scale number and X_1 is zero, so the displacement of the foundation X is the same as the free field motion X_0.

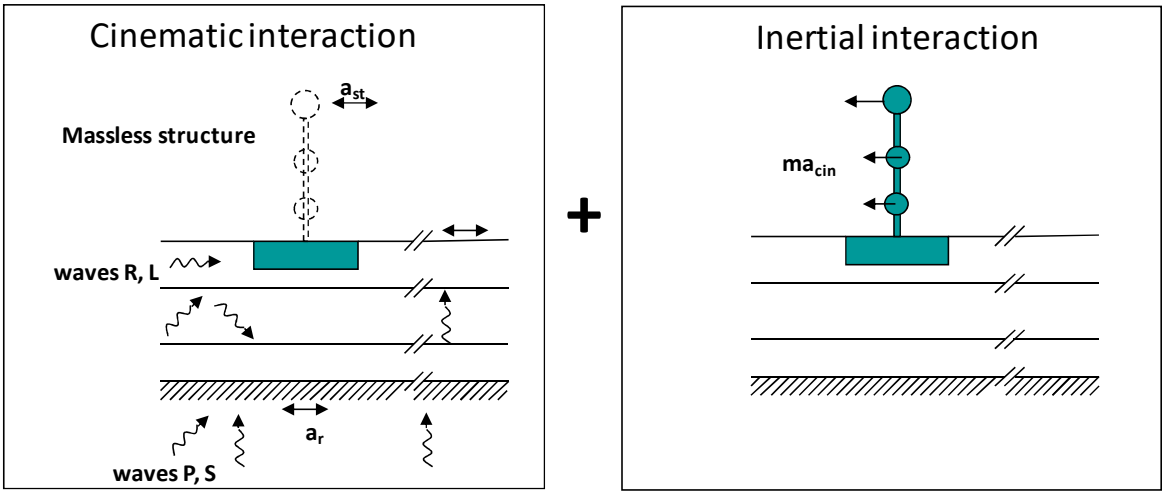

(a) (b)

Figure 1 Sub-structuring method (a) Kinematic interaction; (b) inertial interaction

Substructure approach

SSI problems in dynamic analysis can be solved using a substructure approach, which is composed of three parts independent each other:

1) The first part is finding the FIM by considering the kinematic interaction effect;
2) The second part considers the inertial interaction, in which the impedance function is used;
3) The third part is the dynamic analysis for the structure supported on a compliant base represented by the impedance function, and subjected to a base excitation of FIM;

The kinematic interaction makes the FIM deviate from the free-field motion X_0 because of the existence of a stiff foundation on or in the soil media, which can be caused by

base-slab averaging, embedment/deconvolution effects and wave scattering. Among them, the most significant contribution is given from base-slab averaging and embedment effects. In the inertial interaction consideration, *impedance function* is given as a general expression in the frequency domain as

$$\mathbf{f}_C(\omega) = \mathbf{K}^1(\omega)\mathbf{u}_C(\omega) \tag{1}$$

where $\mathbf{f}_C(\omega) = \begin{bmatrix} f_x & f_y & f_z & m_x & m_y & m_z \end{bmatrix}^T$ is the reaction force-moment vector from the soil media to the foundation when the foundation has a movement $\mathbf{u}_C(\omega) = \begin{bmatrix} u_x & u_y & u_z & \varphi_{ox} & \varphi_{oy} & \varphi_{oz} \end{bmatrix}^T$, and $\mathbf{K^1}(\omega)$ is the matrix of dynamic impedance, which is a 6 × 6 square matrix in a three-dimensional case. Each coefficient K_{prq} of the matrix is in general expressed as the product of a *rigid stiffness K* and of a *dynamic coefficients* $f(\omega)$ which are composed of a real term and an imaginary term as shown below:

$$K_{prq}(\omega) = K \cdot f(\omega) = K\left[k_{prq}(F) + j\omega c_{prq}(F)\right] \tag{2}$$

where $F = \omega B/V_S$ is the dimensionless frequency factor; B is the width of the foundation and V_S is the shear wave velocity; $j = \sqrt{-1}$ and p, q can be *x, y, z.* On the basis of the Fourier transform theory, the real part k_{prq} in the impedance function is the "*dynamic stiffness*" and represents the stiffness and the inertia of the supporting soil; its dependence on frequency is attributed solely to the influence that frequency exerts on inertia, since soil properties are practically frequency independent. The imaginary part c_{prq} is the damping and represents the *radiation* and the *material damping* generated in the system

(due to energy carried by the waves spreading away from the foundation and the energy dissipated in the soil by the hysteretic action, respectively). They can be physically expressed as spring/dashpot pairs with their stiffness and damping coefficient changing with the excitation frequency (Figure 2). The coefficients k_{prq} and c_{prq} are in general evaluated with numerical methods for different soil types [14]. In general, the *matrices of dynamic impedance functions are* provided in dimensionless graphical or tabular forms in the work of Gazetas [14] for an elastic and homogeneous half-space. Equation (2) suggests for each mode of oscillation an analogy between the actual foundation-soil system and the system that consists of the same foundation, but is supported on a spring and dashpot with characteristic moduli equal to k_{prq} and c_{prq}, respectively as the one shown in Figure 2. It is important to mention that the coefficients provided in the paper of Gazetas [14] do not include the soil hysteretic damping β which can be included by simply adding the corresponding material dashpot constant $2\left(\bar{K}/\omega\right)\beta$ to the foregoing (radiation) C value.

Two-dimensional approach

In the analyzed case study, the steady-state response of the two-dimensional structure is determined using the usual structural analysis methods, combined with the *matrix of dynamic impedance functions*. The vertical ground motion is neglected; therefore, the impedance function in Equation (1) can be reduced as

$$\begin{Bmatrix} f_x \\ m_{oy} \end{Bmatrix} = \begin{bmatrix} K_{xx} & K_{xry} \\ K_{yrx} & K_{ry} \end{bmatrix} \begin{Bmatrix} u_x \\ \varphi_{0y} \end{Bmatrix} \tag{3}$$

or in extended form

$$\begin{Bmatrix} F_C \\ M_C \end{Bmatrix} = \begin{bmatrix} k_{xx}(\omega) + j\omega c_{xx}(\omega) & k_{xry}(\omega) + j\omega c_{xry}(\omega) \\ k_{yrx}(\omega) + j\omega c_{yrx}(\omega) & k_{ry}(\omega) + j\omega c_{ry}(\omega) \end{bmatrix} \begin{Bmatrix} x_0 \\ \phi \end{Bmatrix} \tag{4}$$

where x_0 and φ are the horizontal and rocking motions of the foundation, respectively; k_{xx} and c_{xx} represent the frequency dependent stiffness and damping in the horizontal direction; k_{ry} and c_{ry} represent the frequency dependent stiffness and damping for the rocking; and k_{yrx}, k_{xry} and c_{yrx}, c_{xry} represent the coupling terms which are negligibly small in the analyzed case study of shallow foundation (Figure 2).

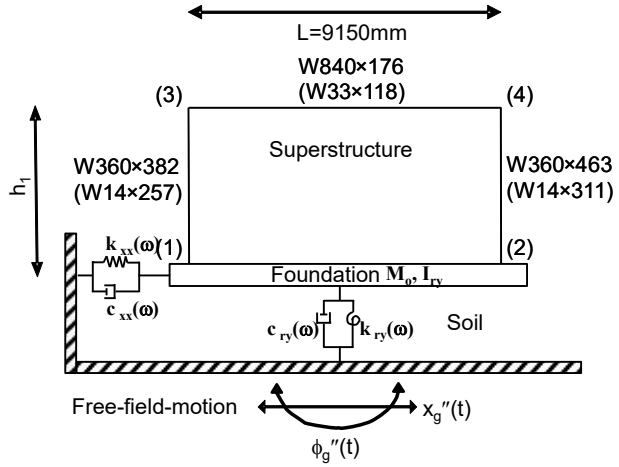

Figure 2 Two-dimensional mathematical model of the SSI structural system

STRUCTURAL FORMULATION OF THE CONTROLLED MDOF SYSTEM WITH SSI

Consider a multi-degree-of-freedom linear building structure equipped with active control systems and subjected to a one-dimensional external excitation considering soil structure interaction as the one shown in Figure 6. The active control is introduced because it will be used to design passive control systems using the methodology

described in the paper of Cimellaro et al. [7]. However, the difference with respect to the fixed base model is that two more degrees of freedom are introduced when the translational and rocking motions of the foundation are included. Furthermore, two more items appear in the inertia forces when the foundation motion is considered. They are $m_i\ddot{x}_0$ and $m_i h_i\ddot{\phi}$ where m_i and h_i are the mass and the height of the ith free body, x_0 is the displacement of the ground at the foundation level. So the *equation of motion of the superstructure* can be obtained by adding those inertial forces to that of the fixed base case as

$$\mathbf{M}\ddot{\mathbf{x}}(t)+\mathbf{M}\boldsymbol{\Gamma}\ddot{\mathbf{x}}_{\mathbf{f}}(t)+\mathbf{C}\dot{\mathbf{x}}(t)+\mathbf{K}\mathbf{x}(t)=\mathbf{H}_{\mathbf{a}}\mathbf{u}(t)+\mathbf{H}_{\mathbf{g}}\mathbf{w}(t) \tag{5}$$

where $\mathbf{x}(t)_{(n\times 1)}$ is the displacement vector relative to the ground; $\ddot{\mathbf{x}}_{\mathbf{f}}^{T}(t)=\left\{\ddot{x}_0(t)\quad \ddot{\phi}_0(t)\right\}_{(1\times 2)}$ is the acceleration vector of the foundation which includes the horizontal and the rocking motion; **M, K** and **C** are the mass, stiffness and inherent damping matrices, respectively; $\mathbf{u}(t)_{r\times 1}$ is the vector of active control forces; $\mathbf{H}_{\mathbf{a}(n\times r)}$ is the location matrix for the active control forces; $\mathbf{w}^{T}(t)=\left\{\ddot{x}_g(t)\quad \ddot{\phi}_g(t)\right\}_{(1\times 2)}$ is the acceleration vector of the ground in term of horizontal and rocking motion; $\mathbf{H}_{\mathbf{g}(n\times 2)}=-\mathbf{M}_{(n\times n)}\boldsymbol{\Gamma}_{(n\times 2)}$ is the base excitation directivity matrix where

$$\boldsymbol{\Gamma}^{T}_{(2\times n)}=\begin{bmatrix}1 & \cdots & 1 & 1\\ h_1 & \cdots & h_{n-1} & h_n\end{bmatrix} \tag{6}$$

is the location matrix of the horizontal and rotational ground motion and h_i is the height of the *i-th* story; n is the number of DOF and r is the number of active control forces. The horizontal-force balance of the free-body foundation is given by

$$m_0\left(\ddot{x}_0+\ddot{x}_g\right)+c_{xx}\dot{x}_0+k_{xx}x_0+F_{up}=0 \tag{7}$$

where F_{up} is the force transferred to the foundation from the superstructure through the columns of the first floor which is given by

$$F_{up}=-c_1\dot{x}_1-k_1x_1=-\begin{bmatrix}1 & 1\ldots & 1\end{bmatrix}_{1\times n}\left(\mathbf{K}\mathbf{x}+\mathbf{C}\dot{\mathbf{x}}\right) \tag{8}$$

where the time dependency has been removed for simplicity. Substituting Equation (5) in Equation (8) it becomes

$$F_{up}=-\begin{bmatrix}1 & 1\ldots & 1\end{bmatrix}_{1\times n}\left(-\mathbf{M}\ddot{\mathbf{x}}(t)-\mathbf{M}\boldsymbol{\Gamma}\ddot{\mathbf{x}}_{\mathbf{f}}(t)+\mathbf{H}_{\mathbf{a}}\mathbf{u}(t)+\mathbf{H}_{\mathbf{g}}\mathbf{w}(t)\right) \tag{9}$$

Since the active control forces are internally acting on the floors, they are self balanced within the superstructure, so they are equal to a null vector, so Equation (10) can be simplified as

$$F_{up}=-\begin{bmatrix}1 & 1\ldots & 1\end{bmatrix}_{1\times n}\left(-\mathbf{M}\ddot{\mathbf{x}}(t)-\mathbf{M}\boldsymbol{\Gamma}\ddot{\mathbf{x}}_{\mathbf{f}}(t)+\mathbf{H}_{\mathbf{g}}\mathbf{w}(t)\right) \tag{10}$$

Substituting Equation (10) in Equation (7) the equation of motion of the foundation in the horizontal direction becomes

$$m_0\left(\ddot{x}_0+\ddot{x}_g\right)-\begin{bmatrix}1 & 1\ldots & 1\end{bmatrix}_{1\times n}\left(-\mathbf{M}\ddot{\mathbf{x}}(t)-\mathbf{M}\boldsymbol{\Gamma}\ddot{\mathbf{x}}_{\mathbf{f}}(t)+\mathbf{H}_{\mathbf{g}}\mathbf{w}(t)\right)+c_{xx}\dot{x}_0+k_{xx}x_0=0 \tag{11}$$

where the first term is the inertial force at the foundation level, the second term represents the force transferred from the superstructure and the last two terms represent the reaction force of the soil to the foundation in the lateral direction. The equation of

rocking motion at the foundation can be obtained by moment balance of the whole system using a similar approach and its expression is given below

$$I_{ry}\left(\ddot{\phi}_0+\ddot{\phi}_g\right)+\begin{bmatrix}h_1 & \dots & h_n\end{bmatrix}_{1\times n}\left(-\mathbf{M}\ddot{\mathbf{x}}(t)-\mathbf{M}\boldsymbol{\Gamma}\ddot{\mathbf{x}}_{\mathbf{f}}(t)+\mathbf{H}_{\mathbf{g}}\mathbf{w}(t)\right)+c_{ry}\dot{\phi}_0+k_{ry}\phi_0=0 \tag{12}$$

where the first term is the inertial moment at the foundation level, the second term represents the moments transferred from the inertial forces at each mass of the superstructure and the last two terms represent the reaction moment of the soil to the foundation. Equation (11) and Equation (12) can be combined to give the final equation of motion for the foundation

$$\begin{bmatrix}m_0 & \\ & I_{ry}\end{bmatrix}\begin{Bmatrix}\ddot{x}_0+\ddot{x}_g\\ \ddot{\phi}_0+\ddot{\phi}_g\end{Bmatrix}+\boldsymbol{\Gamma}^T\left(-\mathbf{M}\ddot{\mathbf{x}}(t)-\mathbf{M}\boldsymbol{\Gamma}\ddot{\mathbf{x}}_{\mathbf{f}}(t)+\mathbf{H}_{\mathbf{g}}\mathbf{w}(t)\right)=-\begin{bmatrix}c_{xx} & \\ & c_{ry}\end{bmatrix}\begin{Bmatrix}\dot{x}_0\\ \dot{\phi}_0\end{Bmatrix}-\begin{bmatrix}k_{xx} & \\ & k_{ry}\end{bmatrix}\begin{Bmatrix}x_0\\ \phi_0\end{Bmatrix} \tag{13}$$

Substituting Equation (5) in Equation (13) the *equation of the foundation* becomes

$$\begin{bmatrix}m_0 & \\ & I_{ry}\end{bmatrix}\begin{Bmatrix}\ddot{x}_0+\ddot{x}_g\\ \ddot{\phi}_0+\ddot{\phi}_g\end{Bmatrix}+\boldsymbol{\Gamma}^T\mathbf{C}\dot{\mathbf{x}}(t)+\begin{bmatrix}c_{xx} & \\ & c_{ry}\end{bmatrix}\begin{Bmatrix}\dot{x}_0\\ \dot{\phi}_0\end{Bmatrix}+\boldsymbol{\Gamma}^T\mathbf{K}\mathbf{x}(t)+\begin{bmatrix}k_{xx} & \\ & k_{ry}\end{bmatrix}\begin{Bmatrix}x_0\\ \phi_0\end{Bmatrix}=\boldsymbol{\Gamma}^T\mathbf{H}_{\mathbf{a}}\mathbf{u}(t) \tag{14}$$

The total floor displacement $\mathbf{x_t}$ relative to the ground when considering SSI is defined as

$$\mathbf{x}_{\mathbf{t}}(t)=\mathbf{x}(t)+\boldsymbol{\Gamma}\mathbf{x}_{\mathbf{f}}(t) \tag{15}$$

where $\mathbf{x}^T_{\mathbf{f}}(t)=\begin{Bmatrix}x_0(t) & \phi_0(t)\end{Bmatrix}_{(1\times 2)}$ is the displacement vector of the foundation which includes the horizontal and the rocking motion. By substituting Equation (15) in Equation (5) and (14) it is obtained

$$\mathbf{M}\ddot{\mathbf{x}}_{\mathbf{t}}(t)-\mathbf{M}\boldsymbol{\Gamma}\ddot{\mathbf{x}}_{\mathbf{f}}(t)+\mathbf{C}\dot{\mathbf{x}}_{\mathbf{t}}(t)-\mathbf{C}\boldsymbol{\Gamma}\dot{\mathbf{x}}_{\mathbf{f}}(t)+\mathbf{K}\mathbf{x}_{\mathbf{t}}(t)-\mathbf{K}\boldsymbol{\Gamma}\mathbf{x}_{\mathbf{f}}(t)=\mathbf{H}_{\mathbf{a}}\mathbf{u}(t)+\mathbf{H}_{\mathbf{g}}\mathbf{w}(t) \tag{16}$$

$$\begin{bmatrix} m_0 & \\ & I_{ry} \end{bmatrix}\ddot{\mathbf{x}}_{\mathbf{f}}+\boldsymbol{\Gamma}^T\mathbf{C}\dot{\mathbf{x}}_{\mathbf{t}}(t)-\left(\boldsymbol{\Gamma}^T\mathbf{C}\boldsymbol{\Gamma}-\begin{bmatrix} c_{xx} & \\ & c_{ry} \end{bmatrix}\right)\dot{\mathbf{x}}_{\mathbf{f}}+\boldsymbol{\Gamma}^T\mathbf{K}\mathbf{x}_{\mathbf{t}}(t)-\left(\boldsymbol{\Gamma}^T\mathbf{K}\boldsymbol{\Gamma}-\begin{bmatrix} k_{xx} & \\ & k_{ry} \end{bmatrix}\right)\mathbf{x}_{\mathbf{f}}=\boldsymbol{\Gamma}^T\mathbf{H}_{\mathbf{a}}\mathbf{u}(t)-\begin{bmatrix} m_0 & \\ & I_{ry} \end{bmatrix}\begin{Bmatrix} \ddot{x}_g \\ \ddot{\phi}_g \end{Bmatrix} \tag{17}$$

The equation of motion of the whole system can be obtained by assembling Equation (16) for the superstructure and Equation (17) for the foundation.

$$\begin{bmatrix} \mathbf{M} & \\ & \mathbf{M}_{\mathbf{f}} \end{bmatrix}\begin{Bmatrix} \ddot{\mathbf{x}}_{\mathbf{t}} \\ \ddot{\mathbf{x}}_{\mathbf{f}} \end{Bmatrix}+\begin{bmatrix} \mathbf{C} & -\mathbf{C}\boldsymbol{\Gamma} \\ \boldsymbol{\Gamma}^T\mathbf{C} & -\boldsymbol{\Gamma}^T\mathbf{C}\boldsymbol{\Gamma}-\mathbf{C}_{\mathbf{s}} \end{bmatrix}\begin{Bmatrix} \dot{\mathbf{x}}_{\mathbf{t}} \\ \dot{\mathbf{x}}_{\mathbf{f}} \end{Bmatrix}+\begin{bmatrix} \mathbf{K} & -\mathbf{K}\boldsymbol{\Gamma} \\ \boldsymbol{\Gamma}^T\mathbf{K} & -\boldsymbol{\Gamma}^T\mathbf{K}\boldsymbol{\Gamma}-\mathbf{K}_{\mathbf{s}} \end{bmatrix}\begin{Bmatrix} \mathbf{x}_{\mathbf{t}} \\ \mathbf{x}_{\mathbf{f}} \end{Bmatrix}=\begin{bmatrix} \mathbf{H}_{\mathbf{a}} \\ \boldsymbol{\Gamma}^T\mathbf{H}_{\mathbf{a}} \end{bmatrix}\mathbf{u}(t)-\begin{bmatrix} \mathbf{M} & \\ & \mathbf{M}_{\mathbf{f}} \end{bmatrix}\begin{bmatrix} \boldsymbol{\Gamma} \\ \mathbf{I}_{\mathbf{2}} \end{bmatrix}\begin{Bmatrix} \ddot{x}_g \\ \ddot{\phi}_g \end{Bmatrix} \tag{18}$$

where

$$\mathbf{M}_{\mathbf{f}}=\begin{bmatrix} m_0 & \\ & I_{ry} \end{bmatrix};\quad \mathbf{C}_{\mathbf{s}}=\begin{bmatrix} c_{xx} & \\ & c_{ry} \end{bmatrix};\quad \mathbf{K}_{\mathbf{s}}=\begin{bmatrix} k_{xx} & \\ & k_{ry} \end{bmatrix};\quad \mathbf{I}_{\mathbf{2}}=\begin{bmatrix} 1 & \\ & 1 \end{bmatrix} \tag{19}$$

By defining the mass, stiffness, damping matrices and input location matrices of the global SSI system

$$\begin{aligned} &\mathbf{M}_{\mathbf{SSI}}=\begin{bmatrix} \mathbf{M} & \\ & \mathbf{M}_{\mathbf{f}} \end{bmatrix}\quad \mathbf{C}_{\mathbf{SSI}}=\begin{bmatrix} \mathbf{C} & -\mathbf{C}\boldsymbol{\Gamma} \\ \boldsymbol{\Gamma}^T\mathbf{C} & -\boldsymbol{\Gamma}^T\mathbf{C}\boldsymbol{\Gamma}-\mathbf{C}_{\mathbf{s}} \end{bmatrix}\quad \mathbf{K}_{\mathbf{SSI}}=\begin{bmatrix} \mathbf{K} & -\mathbf{K}\boldsymbol{\Gamma} \\ \boldsymbol{\Gamma}^T\mathbf{K} & -\boldsymbol{\Gamma}^T\mathbf{K}\boldsymbol{\Gamma}-\mathbf{K}_{\mathbf{s}} \end{bmatrix} \\ &\mathbf{H}_{\mathbf{SSI},a}=\begin{bmatrix} \mathbf{H} \\ -\Gamma_1^T\mathbf{H} \end{bmatrix}\quad \mathbf{H}_{\mathbf{SSI},r}=-\mathbf{M}_{\mathbf{SSI}}\begin{bmatrix} \boldsymbol{\Gamma} \\ \mathbf{I}_{\mathbf{2}} \end{bmatrix} \end{aligned} \tag{20}$$

The general equation of motion of the linear system with active control forces considering SSI in Equation (18) can be simply expressed as

$$\mathbf{M}_{\mathbf{SSI}}\ddot{\mathbf{x}}_t(t)+\mathbf{C}_{\mathbf{SSI}}\dot{\mathbf{x}}_t(t)+\mathbf{K}_{\mathbf{SSI}}\mathbf{x}_t(t)=\mathbf{H}_{\mathbf{SSI},a}\mathbf{u}(t)-\mathbf{H}_{\mathbf{SSI},r}\begin{Bmatrix} \ddot{\mathbf{x}}_g(t) \\ \ddot{\phi}_g(t) \end{Bmatrix} \tag{21}$$

INTEGRATED DESIGN

The two-step solution, defined further as the "*redesign approach*", is then formulated and developed in detail in the paper of Cimellaro et al. [1]. The main idea is simultaneously optimize the structural parameters ξ and the active control forces $\mathbf{u}(t)$ in such a way to minimize an appropriate objective function. The optimization problem can be solved using a two steps procedure. In fact, while traditionally in control of buildings, the structure is designed first and then the controller, the proposed design method reverses the procedure by designing the structure after the controller is given. The fundamental idea of redesign was proposed by Smith et al. [15]. In the paper of Cimellaro et al. [1], the idea of redesign is incorporated into the integrated design of structural/control systems. The procedure is summarized in the following steps:

First step: The desired structure is chosen based on best practice using engineering experience and it is assumed fixed while the controller is designed in order to satisfy a given performance requirement (e.g., drift, absolute acceleration, base shear, etc.) of the initial structure. The dynamic response of the initial structure in this step is called "*Ideal Response*".

Second step: The structure and the controller are then redesigned to achieve a common goal prescribed by the performance obtained in the first step (the ideal dynamic response). The structure is redesigned for better controllability by modifying the structural system and reducing the amount of active control power needed to achieve the "*Ideal Response*".

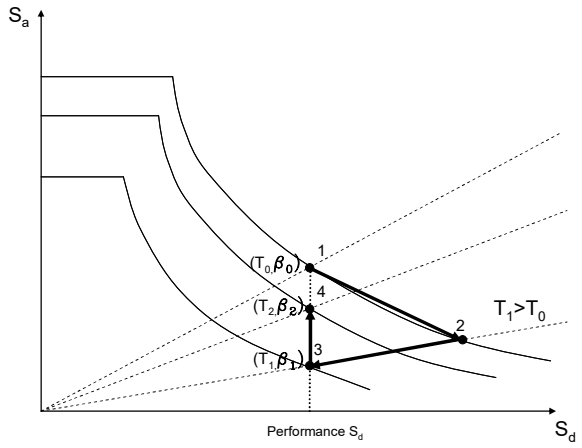

Figure 3 Integrated redesign procedure in Sd-Sa plane

These two steps can be better understood by considering relationship between spectral acceleration and spectral displacement (S_a-S_d) in structural design. In Figure 3 is shown a typical (S_a-S_d) spectrum for several damping levels. $S_d(T_0, \beta_0)$ and $S_a(T_0, \beta_0)$ are the spectral coordinates of the original structure with period T_0 and damping β_0. In *Step 1*, the structure at point 1 is made lighter by reducing its structural mass (weight) and its stiffness and it moves to point 2 in Figure 1. Then a controller is applied to bring back the structure to the initial ideal response at point 3. In *Step 2*, the structure is redesigned in order to achieve the same performance, but with less amount of active control forces or damping. During the redesign, mass, stiffness and damping are modified in order to achieve this goal, reaching finally point 4 in Figure 1. At the end of this step, the building will maintain the same performance, but with less amount of control forces.

Mathematical formulation of the redesign approach

The integrated redesign procedure considering SSI for the case when the building is assumed linear is formulated in this paragraph. In the state space, Equation (21) becomes:

$$\dot{\mathbf{z}}(t) = \mathbf{A}\mathbf{z}(t) + \mathbf{B}\mathbf{u}(t) + \mathbf{e}(t) \tag{22}$$

where

$$\mathbf{z}(t) = \begin{bmatrix} \mathbf{x}(t) \\ \dot{\mathbf{x}}(t) \end{bmatrix};\ \mathbf{e}(t) = \begin{bmatrix} \mathbf{0} \\ -\mathbf{M}_{\mathbf{SSI}}{}^{-1}\mathbf{H}_{\mathbf{SSI},r} \end{bmatrix} \begin{Bmatrix} \ddot{\mathbf{x}}_g(t) \\ \ddot{\phi}_g(t) \end{Bmatrix};\ \mathbf{A} = \begin{bmatrix} \mathbf{0} & \mathbf{I} \\ -\mathbf{M}_{\mathbf{SSI}}{}^{-1}\mathbf{K}_{\mathbf{SSI}} & -\mathbf{M}_{\mathbf{SSI}}{}^{-1}\mathbf{C}_{\mathbf{SSI}} \end{bmatrix};\ \mathbf{B} = \begin{bmatrix} \mathbf{0} \\ \mathbf{M}_{\mathbf{SSI}}{}^{-1}\mathbf{H}_{\mathbf{SSI},a} \end{bmatrix}; \tag{23}$$

Step 1. A control law is employed such that the structural system has acceptable performance such as satisfaction of certain constraints on the dynamic response. Many methods can be used for this purpose (e.g. Linear Quadratic Regulator (LQR), pole assignments, etc, [16]). Using a linear control law, for example, **u(**t**)** can be expressed as:

$$\mathbf{u}(t) = \mathbf{G}\mathbf{z}(t) \tag{24}$$

where **G** is the gain matrix that can be obtained from the solution of the Ricatti equation. It is important to note that LQR implies optimality for a white noise excitation, assumption leading to Ricatti equation and its solution. For any other motion, this is sub-optimal [17]. However, the controllers designed using LQR were proven efficient in practical applications for seismic protection [18][19]. Moreover, the active control forces obtained for each DOF considered in the design procedure can be easily converted to equivalent passive devices using a method described in Lavan *et al*. [8] and Cimellaro *et al*. [7].

Step 2. Following Step1, the redesign concept is to change the mass, stiffness, damping matrices, respectively, by **ΔM**, **ΔK** and **ΔC**, and to determine the control force **u** so that the new system becomes

$$(\mathbf{M}_{\mathbf{SSI}} + \Delta\mathbf{M})\ddot{\mathbf{x}}(t) + (\mathbf{C}_{\mathbf{SSI}} + \Delta\mathbf{C})\dot{\mathbf{x}}(t) + (\mathbf{K}_{\mathbf{SSI}} + \Delta\mathbf{K})\mathbf{x}(t) = \mathbf{H}_{\mathbf{SSI},a}\mathbf{u}_a(t) - \mathbf{H}_{\mathbf{SSI},r} \begin{Bmatrix} \ddot{\mathbf{x}}_g(t) \\ \ddot{\phi}_g(t) \end{Bmatrix} \tag{25}$$

where

$$\mathbf{u}_a(t) = \mathbf{G}_a \mathbf{z}(t) \tag{26}$$

where $\mathbf{G_a}$ is the active part of the controller after redesign. The main idea is to separate the control law, Equation (24), into a passive part which is implemented into the physical system by redesign, and an active part which constitutes the remaining active control law required after structure redesign. Therefore, the control law is written in the following form:

$$\mathbf{H}_{\mathbf{SSI},a}\mathbf{u}(t) = \mathbf{H}_{\mathbf{SSI},a}\mathbf{G}\begin{bmatrix}\mathbf{x}(t)\\ \dot{\mathbf{x}}(t)\end{bmatrix} = \mathbf{H}_{\mathbf{SSI},a}\mathbf{G}_a\begin{bmatrix}\mathbf{x}(t)\\ \dot{\mathbf{x}}(t)\end{bmatrix} - \begin{bmatrix}\Delta\mathbf{K} & \Delta\mathbf{C}\end{bmatrix}\begin{bmatrix}\mathbf{x}(t)\\ \dot{\mathbf{x}}(t)\end{bmatrix} - \Delta\mathbf{M}\ddot{\mathbf{x}}(t) \tag{27}$$

and the closed-loop system after redesign is

$$(\mathbf{M}_{\mathbf{SSI}} + \Delta\mathbf{M})\ddot{\mathbf{x}}(t) + (\mathbf{C}_{\mathbf{SSI}} + \Delta\mathbf{C})\dot{\mathbf{x}}(t) + (\mathbf{K}_{\mathbf{SSI}} + \Delta\mathbf{K})\mathbf{x}(t) = \mathbf{H}_{\mathbf{SSI},a}\mathbf{G}_a\mathbf{z}(t) - \mathbf{H}_{\mathbf{SSI},r}\begin{Bmatrix}\ddot{\mathbf{x}}_g(t)\\ \ddot{\phi}_g(t)\end{Bmatrix} \tag{28}$$

where $\mathbf{u}_a(t)$, which is given by the Equation (26), is the active part of the controller and $\Delta\mathbf{M}\ddot{\mathbf{x}}(t) + \Delta\mathbf{C}\dot{\mathbf{x}}(t) + \Delta\mathbf{K}\mathbf{x}(t)$ is the passive part. The objective of the redesign is to find the passive control ($\mathbf{\Delta M, \Delta K, \Delta C}$) in order to minimize the control power needed to satisfy Equation (27) for any given $\mathbf{G}$. Note that the closed-loop system response before and after redesign remains unchanged; therefore, all the designed closed-loop system properties remain unchanged. Let $\mathbf{B_k}$, $\mathbf{B_c}$ and $\mathbf{B_m}$ be the stiffness, damping and mass connectivity matrices of the structural system. The changes in the structural parameters can be expressed in the form:

$$\begin{aligned}\Delta\mathbf{K} &= \mathbf{B}_\mathbf{k}\mathbf{G}_\mathbf{k}\mathbf{B}_\mathbf{k}^\mathbf{T}\\ \Delta\mathbf{C} &= \mathbf{B}_\mathbf{c}\mathbf{G}_\mathbf{c}\mathbf{B}_\mathbf{c}^\mathbf{T}\\ \Delta\mathbf{M} &= \mathbf{B}_\mathbf{m}\mathbf{G}_\mathbf{m}\mathbf{B}_\mathbf{m}^\mathbf{T}\end{aligned} \tag{29}$$

where

$$\begin{aligned}\mathbf{G_k} &= diag\left(\ldots,\Delta k_i,\ldots\right)\\ \mathbf{G_c} &= diag\left(\ldots,\Delta c_i,\ldots\right)\\ \mathbf{G_m} &= diag\left(\ldots,\Delta m_i,\ldots\right)\end{aligned} \tag{30}$$

Substituting the solution of $\ddot{\mathbf{x}}(t)$ from Equation (21), into Equation (27) yields:

$$\mathbf{H_{SSI,a}Gz}(t) = \left(\mathbf{G}_{active} + \mathbf{G}_{passive}\right)\mathbf{z}(t) \tag{31}$$

where

$$\mathbf{G}_{active} = \mathbf{H_{SSI,a}G}_a \tag{32}$$

$$\mathbf{G}_{passive} = \mathbf{-I_0B_pG_pB_p^TL} \tag{33}$$

with

$$\mathbf{B_p} = \begin{bmatrix} B_k & 0 & 0\\ 0 & B_c & 0\\ 0 & 0 & B_m\end{bmatrix},\ \mathbf{G_p} = \begin{bmatrix} G_k & 0 & 0\\ 0 & G_c & 0\\ 0 & 0 & G_m\end{bmatrix},\ \mathbf{I_0} = \begin{bmatrix} I & I & I\end{bmatrix}, \tag{34}$$

and

$$\mathbf{L} = \begin{bmatrix} \mathbf{I}\\ \mathbf{M_{SSI}}^{-1}\left(\mathbf{H_{SSI,a}G} - \begin{bmatrix}\mathbf{K_{SSI}} & \mathbf{C_{SSI}}\end{bmatrix}\right)\end{bmatrix} \tag{35}$$

The necessary and sufficient condition to resolve the control law into an active and a passive part as in Equation (31), it is given as follows.

Lemma 1: There exists an active controller G_a satisfying [15]:

$$\mathbf{H_{SSI,a}G} = \mathbf{H_{SSI,a}G}_a - \mathbf{I_0B_pG_pB_p^TL} \tag{36}$$

if and only if:

$$\mathbf{H_{SSI,a}H_{SSI,a}}^{+}\mathbf{I_0B_pG_pB_p^TL} = \mathbf{I_0B_pG_pB_p^TL} \tag{37}$$

and, if this condition is satisfied, $\mathbf{G_a}$ is given by:

$$\mathbf{G}_a = \mathbf{G} + \mathbf{I_0}\mathbf{B_p}\mathbf{G_p}\mathbf{B_p^T}\mathbf{L} \tag{38}$$

where $(\,)^+$ denotes the Moore-Penrose inverse of a matrix. For the passive control law to be physically implemented, it must satisfy certain inequality constraints due to the physics of the problem. For example, the stiffness and the damping of any element of the system after redesign cannot be negative, while the weight of any element cannot be below a certain threshold, without compromising the stability of the structure. Then if $\mathbf{C}$=diag[k_i,..c_i,…m_i,…] is a matrix with diagonal elements containing the specified lower bound values of the structural elements after redesign and $\mathbf{S}$= diag[$_{k0i}$,..c_{0i},…m_{0i},…] is the matrix of the initial parameters, then these constraints can be presented as:

$$\mathbf{G}_p + \mathbf{S} \geq \mathbf{C} \tag{39}$$

The objective function being minimized can be the square of the active part of the control law given by:

$$F\left(\mathbf{G_p}\right) = \int \mathbf{u}_a^T(t)\mathbf{R}\mathbf{u}_a(t)dt = trace\left(\mathbf{G_a}\mathbf{R_{XX}}\mathbf{G_a^T}\mathbf{R}\right) \tag{40}$$

where $\mathbf{R_{XX}}$ is the covariance matrix of the response. Finally the formulation of the optimization problem is:

$$\text{minimize} \quad F\left(\mathbf{G_p}\right) = trace\left(\mathbf{G_a}\mathbf{R_{XX}}\mathbf{G_a^T}\mathbf{R}\right) \tag{41}$$

where $\mathbf{G_a}$ is given by Equation (38), subjected to the equality constraints of Equation (37) and inequality constraint in Equation (39). An approach to solving numerically the constrained optimization problem is to use the "*Exterior penalty function method*" that is part of the Sequential Unconstrained Minimization Techniques (SUMT) [20]. This

requires the solution of several unconstrained minimization problems. The approach consists of creating an unconstrained objective function of the form:

$$\Phi\left(\mathbf{G_p}, r_p\right) = F\left(\mathbf{G_p}\right) + r_p P\left(\mathbf{G_p}\right) \tag{42}$$

where $F(\mathbf{G_p})$ is the original objective function, $P(\mathbf{G_p})$ is the penalty function and r_p is a multiplier which determines the magnitude of the penalty and it is held constant during a complete unconstraint minimization. The penalty function $P(\mathbf{G_p})$ is given by the following expression in this case:

$$P\left(\mathbf{G_p}\right) = trace\left[\mathbf{Z}\left(\mathbf{G_P} + \mathbf{S} - \mathbf{C}\right)\left(\mathbf{G_P} + \mathbf{S} - \mathbf{C}\right)^T\right] + trace\left\{\left(\mathbf{B}\mathbf{B}^{+}\mathbf{I_0}\mathbf{B_p}\mathbf{G_p}\mathbf{B_p^T}\mathbf{L}\mathbf{H}_{\mathbf{SSI},a}\mathbf{H}_{\mathbf{SSI},a}{}^{+} - \mathbf{I_0}\mathbf{B_p}\mathbf{G_p}\mathbf{B_p^T}\mathbf{L}\right)\times \left(\mathbf{B}\mathbf{B}^{+}\mathbf{I_0}\mathbf{B_p}\mathbf{G_p}\mathbf{B_p^T}\mathbf{L}\mathbf{H}_{\mathbf{SSI},a}\mathbf{H}_{\mathbf{SSI},a}{}^{+} - \mathbf{I_0}\mathbf{B_p}\mathbf{G_p}\mathbf{B_p^T}\mathbf{L}\right)^T\right\} \tag{43}$$

where $\mathbf{Z}$=diag(…z_i…) is a diagonal matrix where the scalars z_i are chosen such that z_i=1 if the corresponding inequality constraint $G_{pi}+s_i-c_i \geq 0$ is active, and z_i=0 if the constraint is not active. Therefore, the new objective function is given by the following expression:

$$\Phi\left(\mathbf{G_p}, r_p\right) = trace\left(\mathbf{G_a}\mathbf{R_{XX}}\mathbf{G_a^T}\mathbf{R}\right) + r_p trace\left[\mathbf{Z}\left(\mathbf{G_P} + \mathbf{S} - \mathbf{C}\right)\left(\mathbf{G_P} + \mathbf{S} - \mathbf{C}\right)^T\right] +$$

$$r_p trace\left\{\left(\mathbf{B}\mathbf{B}^{+}\mathbf{I_0}\mathbf{B_p}\mathbf{G_p}\mathbf{B_p^T}\mathbf{L}\mathbf{H}_{\mathbf{SSI},a}\mathbf{H}_{\mathbf{SSI},a}{}^{+} - \mathbf{I_0}\mathbf{B_p}\mathbf{G_p}\mathbf{B_p^T}\mathbf{L}\right)\left(\mathbf{B}\mathbf{B}^{+}\mathbf{I_0}\mathbf{B_p}\mathbf{G_p}\mathbf{B_p^T}\mathbf{L}\mathbf{H}_{\mathbf{SSI},a}\mathbf{H}_{\mathbf{SSI},a}{}^{+} - \mathbf{I_0}\mathbf{B_p}\mathbf{G_p}\mathbf{B_p^T}\mathbf{L}\right)^T\right\} \tag{44}$$

Minimization of equation (44) requires that the following first-order necessary condition is satisfied.

$$\mathbf{P_1}\ vect\ diag\left(\mathbf{G_p}\right) = \mathbf{r_1} \tag{45}$$

where *vec diag*($\mathbf{G_p}$) denotes a vector with diagonal elements of $\mathbf{G_p}$ as its components. We have

$$\mathbf{P}_1 = \left(\mathbf{B}_p^T\mathbf{I}_0^T\mathbf{B}^{+T}\mathbf{R}\mathbf{B}^+\mathbf{I}_0\mathbf{B}_p\right)\circ\left(\mathbf{B}_p^T\mathbf{L}\mathbf{H}_{SSI,a}{}^+\mathbf{H}_{SSI,a}\mathbf{R}_{XX}\mathbf{H}_{SSI,a}{}^+\mathbf{H}_{SSI,a}\mathbf{L}^T\mathbf{B}_p\right)+r_p\left(\mathbf{B}_p^T\mathbf{I}_0^T\mathbf{I}_0\mathbf{B}_p\right)\circ \\ \circ\left(\mathbf{B}_p^T\mathbf{L}\mathbf{H}_{SSI,a}{}^+\mathbf{H}_{SSI,a}\mathbf{L}^T\mathbf{B}_p\right)-r_p\left(\mathbf{B}_p^T\mathbf{I}_0^T\mathbf{B}\mathbf{B}^+\mathbf{I}_0\mathbf{B}_p\right)\circ\left(\mathbf{B}_p^T\mathbf{L}\mathbf{H}_{SSI,a}{}^+\mathbf{H}_{SSI,a}\mathbf{L}^T\mathbf{B}_p\right)+\mathbf{Z} \quad (46)$$

and

$$\mathbf{r}_1 = \text{vec diag}\left(\mathbf{B}_p^T\mathbf{I}_0^T\mathbf{B}^{+T}\mathbf{R}\mathbf{G}\mathbf{H}_{SSI,a}\mathbf{R}_{XX}\mathbf{H}_{SSI,a}{}^+\mathbf{H}_{SSI,a}\mathbf{L}^T\mathbf{B}_p\right)-r_p\mathbf{Z}\text{vec diag}(\mathbf{S}-\mathbf{C}) \quad (47)$$

Therefore, the following algorithm can be used to find the optimal solution, where it is assumed that the matrix P_1 is invertible. If a small value of r_p is chosen, the resulting function $\Phi(\mathbf{G}_P, r_p)$ is easily minimized, but may yield large constraints violations. On the other hand, a large value of r_p will ensure near satisfaction of all constraints but will create a very poorly conditioned optimization problem from a numerical standpoint. Therefore, the algorithm starts with a small value of r_p and minimize $\Phi(\mathbf{G}_P, r_p)$. Then r_p is increased by a factor γ, say γ=3, and $\Phi(\mathbf{G}_P, r_p)$ is minimized again, each time beginning the optimization from the previous solution, until a satisfactory result is obtained.

CASE STUDY

SDOF steel portal frame with SSI

Consider a 2-D moment resisting one-story and one-bay steel frame (Figure 4). The frame consists of two columns (W14×257 and W14×311) and one beam (W33×118). The columns are 345 MPA (50ksi) steel and the beam is 248 MPA (36ksi). The bay width L is 9.15m (30ft) and the height h is 3.96m (13 ft). The frame is subjected to a zero-mean white noise stationary horizontal base acceleration with peak ground acceleration of 1.0 g. The mass is *M=159450 kg* the stiffness is *K=76987 kN/m* and the damping coefficient is *C= 140 kN sec/m* that is determined assuming a Rayleigh damping

equal to *2%*. The period of the uncontrolled frame is $T_0 = 0.28\ sec$. The required lateral stiffness K_s necessary for supporting the gravity loads is:

$$K_s = 0.18K \tag{48}$$

The frame has been designed in order to limit the drift to 0.5% ($x_{lim}=1.98cm$). Following *Step 1*, it considered now a possible reduction of K by introducing a diagonal active brace member while maintaining the original performance level (0.5% drift). Mass will be changed accordingly while damping reduces according to Rayleigh damping constraint. If K_a is the achievable stiffness in the columns of the active structure, Figure 5 shows the value of K_a as a function of the required maximum control force u_{MAX}.

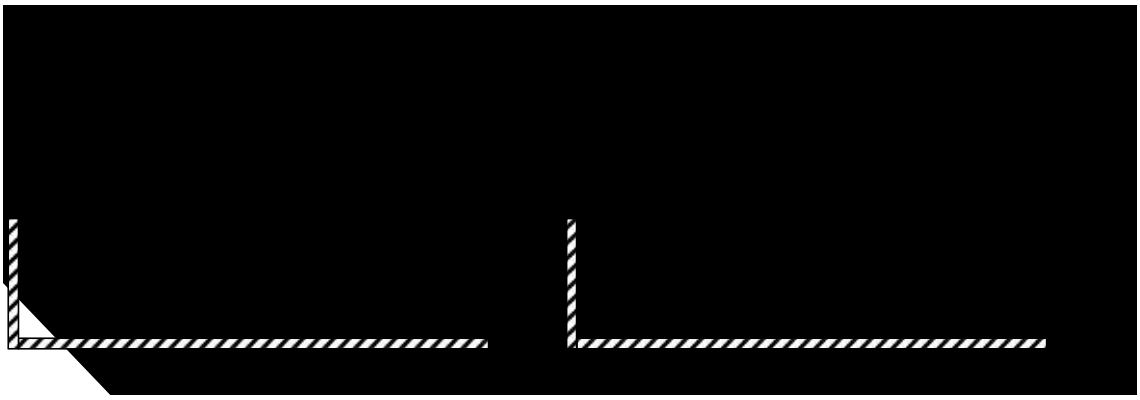

Figure 4 SDOF steel frame with SSI before and after redesign

In particular, it is possible to choose K_a while the dynamic requirements are satisfied entirely through activation of the active brace. In this example, a reduction of stiffness of 60% is selected to satisfy the same performance level of 0.5% drift with a maximum active control force for each soil type which is given in Table 1:

Table 1. Active control force for different soil types and foundation lengths

	Soil Type				
Umax (kN)	A	B	C	D	E
L/B=1	192.4	192.4	191.9	186.6	161.9
L/B=2	192.5	192.5	192.7	206.6	174.4
L/B=4	192.5	192.7	193.4	209.9	198.9
L/B=10	192.5	192.8	194.2	213.1	202.8

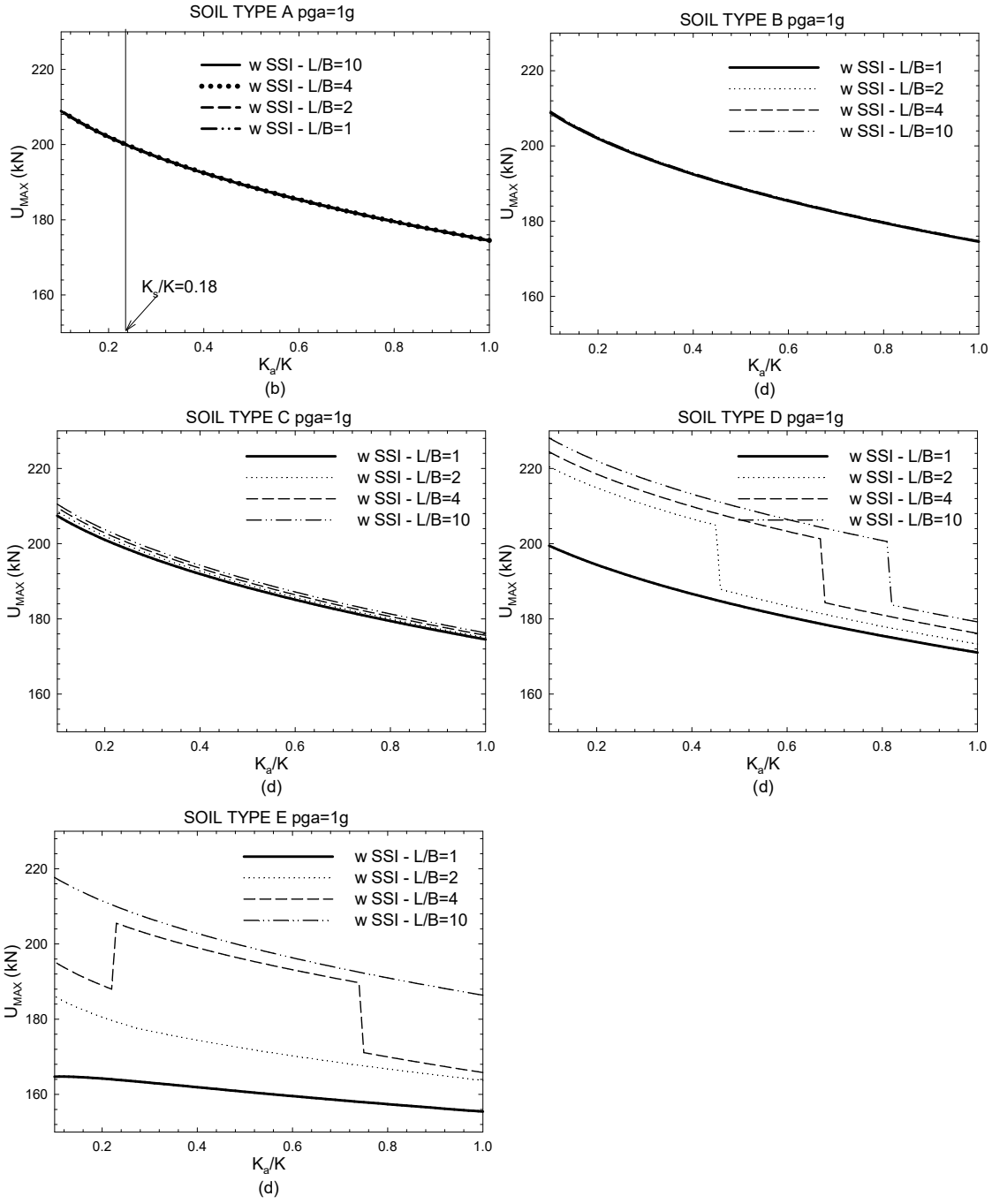

Figure 5 Maximum control force vs. normalized structural stiffness for different soil types and surface foundation dimensions

Many combinations are possible in determining the section properties of the columns and the beam for which it is possible to obtain a stiffness reduction of about 60%. In this example, the two columns are substituted by two *W14×99*. Using this selection, it is possible to obtain a reduction of stiffness of *61.8%* and the new updated stiffness is $K_a = 29401.127\ \text{kN/m}$, while the initial structural steel mass (weight) of the frame is $M_{S0} = 4959.5\text{kg}\ (10924\text{lb})$. With added active brace, the structural steel mass is $M_S = 2775.7\text{kg}\ (6114\text{lb})$. Consequently, the structural steel weight is reduced by 44% by adding an active brace with a maximum control force which range from *162 to 213 kN*, depending on the soil type and the foundation length (Figure 5). For relatively stiff soil (*A, B* and *C*) the length variation of the surface foundation does not change the value of the active control force, therefore the redesign procedure is not affected. For softer soil (*D, E*) increasing the length of the foundation can instead have a negative impact on the value of the active control force which can increase of about 14% for soil type *D* and of about 25% for soil type *E (*Figure 5*d-e)*. In Table 1 can also be observed that the same integrated redesign can be achieved with less control force in the lateral brace, when soft soil are considered for the case of squared foundations, while the trend is the opposite for long foundations (*L/B=10*).

6 story MDOF steel structure with SSI

The controlled building and its characteristic are illustrated in Figure 6. The main difference is that the equation of motion of the superstructure can be obtained for the SSI case by adding the foundation inertial forces to that of the fixed base case. Details about

the derivation of the equation of motion for the 2D-dimensional shear-type building with SSI can be found in Franklin and Cheng [21].

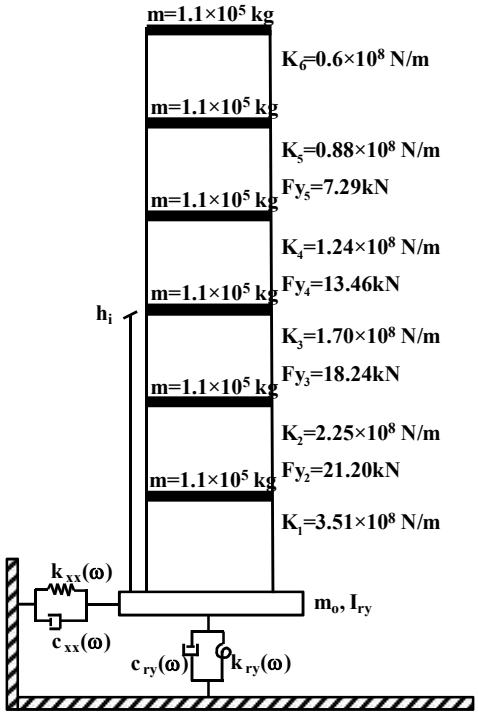

Figure 6 Shear-type model of the MDOF system

The foundation of the building is square with dimensions $12\times12\ m$, mass of $2.2\times10^5 kg$. Different soil conditions are considered and their respective parameters are given below:

Table 2. Parameters of the different soil types

Soil Type	Seismic Velocity at the site V_s (m/s)	Density ρ (kg/m^3)	Shear wave velocity G (MPa)	Coefficient of Poisson v	Geological material
A	1700	2800	8092	0.5	e.g. Crystalline metamorphic rock or not altered
B	1125	2400	3038	0.4	e.g. Limestone
C	550	1690	511	0.2	e.g. Medium sand near the surface
D	275	1430	108	0.3	e.g. Consistent Clay
E	100	1250	13	0.3	e.g. Loose sand

The building is subjected to El Centro Earthquake. The maximum inter-story drift (Figure 7b), absolute acceleration (Figure 7c) and base shear (Figure 7c) normalized with respect to the fixed base condition are shown for different soil types and different foundation lengths. Figure 7 shows that for soft soil (Type E) squared surface foundations (L/B=1) generate a reduction of the structural response of about 10% in term of drift, 20% in term of acceleration and about 40% in term of base shear. Then an optimal damping distribution has been selected using a simple heuristic search approaches called "Sequential Search" [22] which can be easily integrated in conventional design procedures used by practicing engineers dealing with damper-added structures, and they yield a solution which may be close to the optimal solution. The objective function which has been minimized using the algorithm is the maximum inter-story drift. First, preliminary design was performed assuming 25% damping ratio on the first mode assuming one damper placed at every story unit (Uniform distribution) and then the optimization algorithm was applied to the fixed base structure. The resulting optimal damping distribution is a uniform distribution, but with two dampers on the first floor and

none in the last floor. The structural damped response considering SSI is shown in Figure 8.

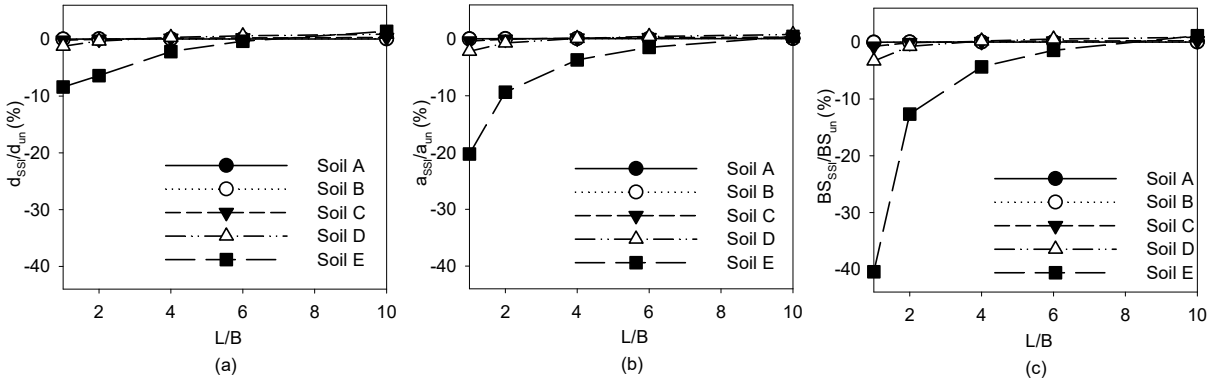

Figure 7 Maximum drift, acceleration and base shear response vs. different foundations extensions and Soil Types for six story uncontrolled building

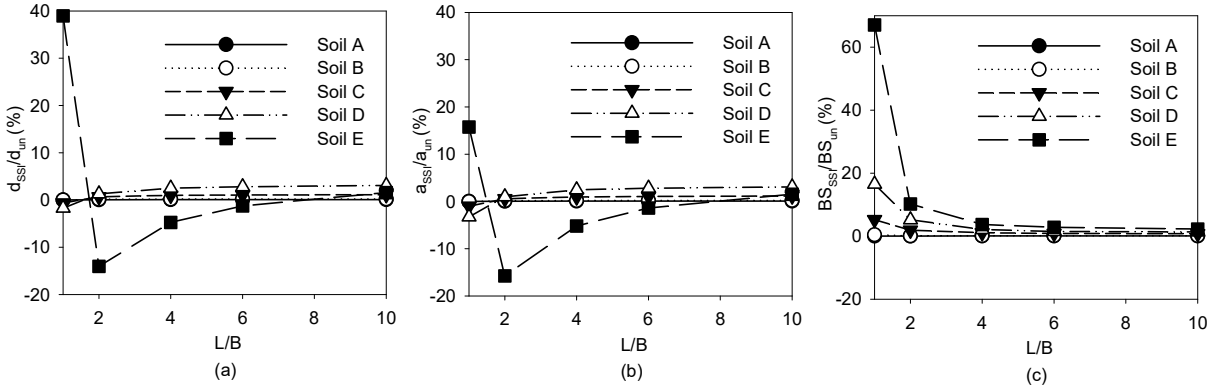

Figure 8 Maximum drift, acceleration and base shear response vs. different foundations extensions and Soil Types for six story damped building

It is shown that the optimal damping distribution selected for the fixed base case provides not conservative results when SSI in not considered. In particular for soft soil (Type E) and squared surface foundations (L/B=1) the drift increases of about 40%, the

accelerations of about 15% and the base shear of about 65% with respect to the fixed base damped configuration.

9 story MDOF steel structure with SSI

The nine-story benchmark structure [23] considered in this example is 45.73 m (150 ft) by 45.73 m (150 ft) in plan, and 37.19 m (122 ft) in elevation. The bays are 9.15 m (30 ft) on center, in both directions, with five bays each in the North-South (N-S) and East-West (E-W) directions. The building's lateral load-resisting system is comprised of steel perimeter moment-resisting frames (MRFs) with simple framing on the furthest south E-W frame. The interior bays of the structure contain simple framing with composite floors. Typical floor-to-floor heights (measured from center-of-beam to center-of-beam for analysis purposes) are 3.96 m (13 ft). The floor-to-floor height of the basement level is 3.65 m (12 ft) and for the first floor is 5.49 m (18 ft). The floor system is comprised of 248 MPa (36 ksi) steel wide-flange beams acting compositely with the floor slab, each frame resisting one-half of the seismic mass associated with the entire structure. The seismic mass at the ground level is 9.65×10^5 *kg (66.0 kip-sec2/ft),* 1.01×10^6 *kg (69.0 kips-sec2/ft)* for the first level, 9.89×10^5 *kg (67.7 kip-sec2/ft)* for the second through eighth levels and 1.07×10^6 *kg (73.2 kip-sec2/ft)* for the ninth level. The seismic mass of the above ground levels of the entire structure is 9.00×10^6 *kg (616 kip-sec2/ft)*. The first three natural frequencies are *0.44*, *1.18* and *2.05* Hz. More details about the model can be found in Othori et al. (2004). Without loss of generality, an equivalent shear-type model is determined by minimizing the difference between the frequencies and the mode shapes of the finite element model and the shear-type model in order to reduce the number of DOFs involved in the methodology. Rayleigh proportional damping is

considered, including *2%* of damping ratio for the first two modes. The structure is subjected to the first *30 sec* of white noise with amplitude of *0.15g* and with a sampling frequency of *0.02 sec*. The coefficient *p* of the *R* matrix [1], is assumed equal to 11.6 to obtain a maximum drift below 1.0% when excited with a white noise of 0.15g of amplitude. After the structure and the controller are designed independently in Step 1, the controller and the building are redesigned together in Step 2 to achieve the same performance (Ideal Response) by reducing the amount of active control power. The percentage of reduction of the total energy transferred to the structure from the controller is given in Table 3.

Table 3. Percentage of reduction of energy transferred to the structure after redesign

Fixed base	A	B	C	D	E
-18.5%	-9%	-6.9%	-12.6%	-10.1%	-7.1%

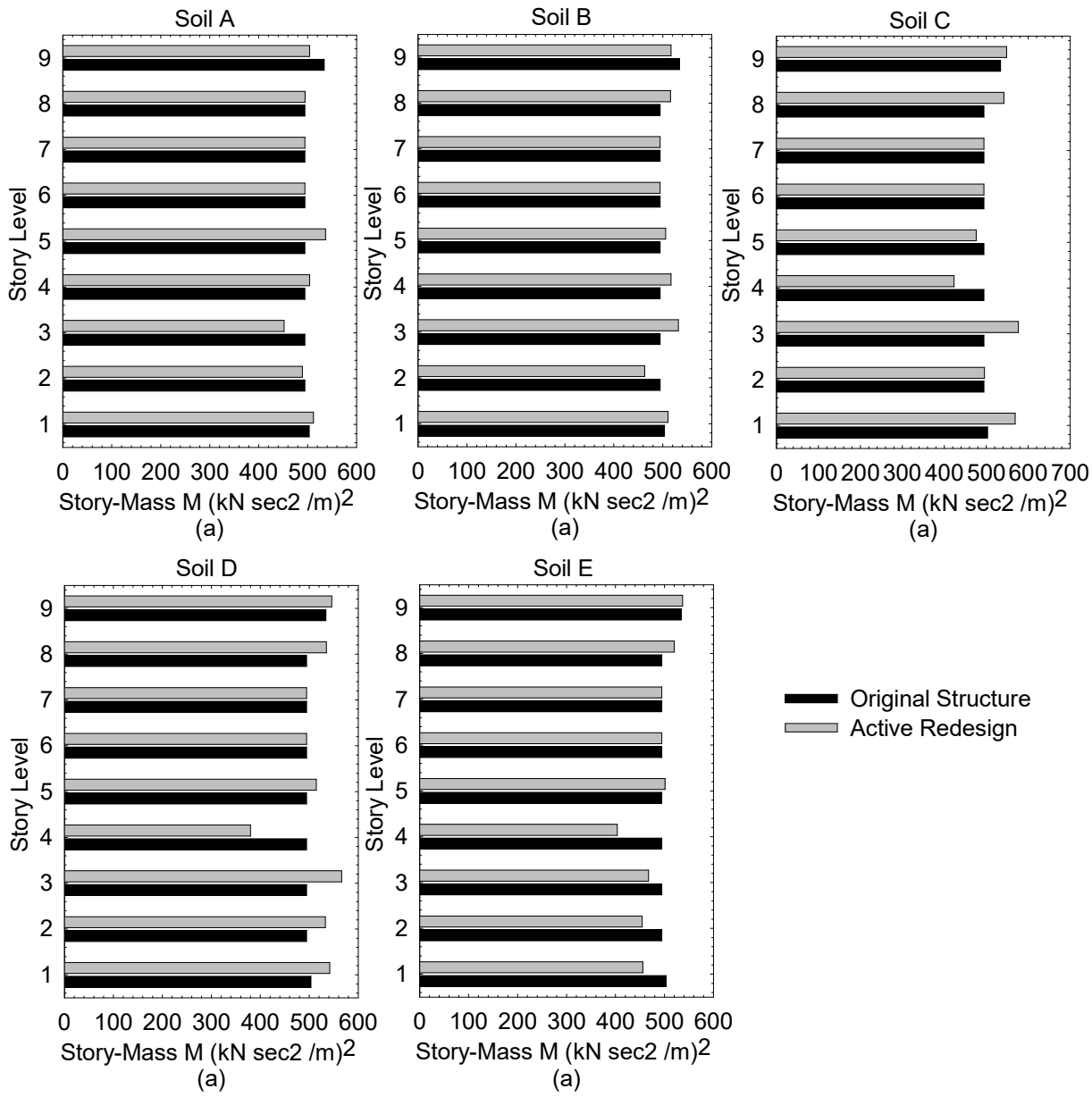

Figure 9 Structural mass Ms before and after redesign of MRF for different soil types

Finally, the story mass distributions before and after redesign for different soil types are shown in Figure 9, where it can be observed a diffused reduction of the structural mass, while the reduction of mass that was obtained with the fixed base case at the upper story levels [1] is no more observed. The total mass reduction for different soil type after the

application of the integrated redesign is shown in Figure 10, where it is observed that for soil type B, C, and D the structural mass actually increases, while reduction has been observed on soil type E. The results above draw the conclusion that SSI should be included in the Integrated Redesign, because in certain cases the design obtained for the fixed base case can bring to not conservative results.

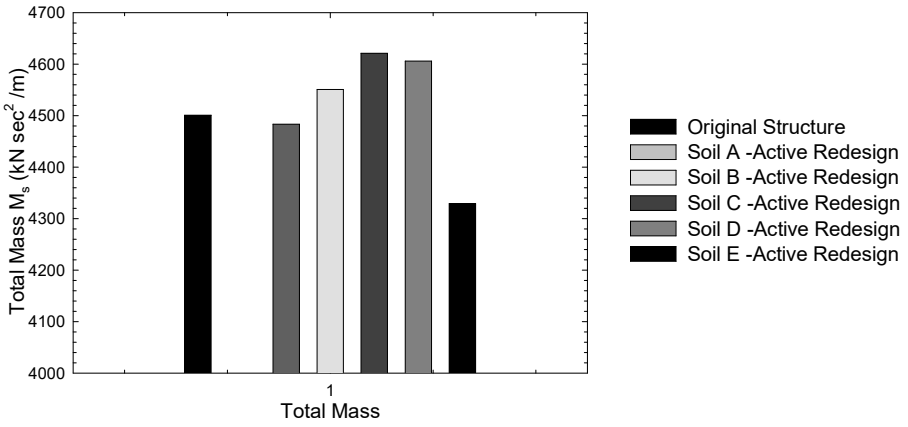

Figure 10 Total mass reduction for different soil types after redesign

CONCLUDING REMARKS

Integrated Redesign has shown its effectiveness in optimizing both the controller and the structure simultaneously, by reducing the structural mass of the building. However past research was applied to fixed based structures considering relatively stiff soil conditions. This paper examines the effects of soil-structure interaction on the seismic performance of integrated redesign. A linear SDOF steel portal frame, a 6 story building and a linear 9-DOF shear-type structure with different soil types and with a rigid surface foundation have been considered to analyze soil-structure interaction effects. For the *single portal frame* with a soft soil (*D, E*) if the length of the foundation increases it can have a negative impact on the active control force which can increase of about 14% for soil type

D and of about 25% for soil type *E*. It is also observed that the same integrated redesign can be achieved with less control force in the lateral brace, when soft soil are considered for the case of squared foundations, while the trend is the opposite for long foundations (L/B=10). For the *six story building* if the optimal damping distribution is obtained from the fixed base case, it can provide larger interstory drifts (+40%) and larger base shear (+65%) with respect to the fixed base case when SSI is considered. The optimal redesign approach on fixed base of a *9 story building* causes a mass reduction on the upper stories, which is not observed when soil structure interaction is included in the model. These observations bring to the conclusions that SSI should be included in the Integrated Redesign approach to determine the optimal damping distribution, otherwise in certain cases unconservative results might be obtained. However, further investigations are necessary to draw more general conclusions.

ACKNOWLEDGMENTS

The research leading to these results has received funding from the European Research Council under the Grant Agreement n° ERC_IDEal reSCUE_637842 of the project IDEAL RESCUE - Integrated DEsign and control of Sustainable CommUnities during Emergencies

REFERENCES

[1] Cimellaro GP, Soong TT, Reinhorn AM. Integrated Design of Controlled Linear Structural Systems. *Journal of Structural Engineering, ASCE*, 2009a; **135** (7): 853-862.

[2] Onoda J, Haftka RT. An approach to structure/control simultaneous optimization for largeflexible spacecraft. *AIAA Journal*, 1987; **25** (8): 1133-1138.

[3] Salama M, Garba J, Demsetz L, Udwadia F. Simultaneous optimization of controlled structures. *Computational Mechanics*, 1988; **3** (4): 275-282.

[4] Curadelli O, Amani M. Integrated structure-passive control design of linear structures under seismic excitations. *Engineering Structures*, 2014; **81**: 256-264.

[5] Xu B. Integrated optimization of structure and control systems for interconnected building structures subjected to earthquake. *Journal of Vibration and Control*, 2014; **20** (9): 1318-1332.

[6] Viti S, Cimellaro GP, Reinhorn AM. Retrofit of a hospital through strength reduction and enhanced damping *Smart Structures and Systems, An international Journal*, 2006; **2** (4): 339-355.

[7] Cimellaro GP, Lavan O, Reinhorn AM. Design of Passive systems for controlled inelastic structures. *Earthquake Engineering & Structural Dynamics*, 2009; **38** (6): 783-804.

[8] Lavan O, Cimellaro GP, Reinhorn AM. Noniterative Optimization Procedure for Seismic Weakening and Damping of Inelastic Structures. *Journal of Structural Engineering*, 2008; **134** (10): 1638-1648.

[9] Cimellaro GP, Lopez-Garcia D. Algorithm for design of controlled motion of adjacent structures. *Journal of Structural control and Health Monitoring*, 2011; **18** (2): 140-148.

[10] Cimellaro GP, Soong TT, Reinhorn AM. Integrated design of inelastic controlled structural systems. *Journal of Structural control and Health Monitoring*, 2009b; **16** (7-8): 689-702.

[11] Sarlis AA, Pasala DTR, Constantinou MC, Reinhorn AM, Nagarajaiah S, Taylor DP. Negative Stiffness Device for Seismic Protection of Structures. *Journal of Structural Engineering*, 2013; **139** (7): 1124-1133.

[12] Pasala DTR, Sarlis AA, Reinhorn AM, Nagarajaiah S, Constantinou MC, Taylor D. Apparent Weakening in SDOF Yielding Structures Using a Negative Stiffness Device: Experimental and Analytical Study. *Journal of Structural Engineering*, 2015; **141** (4): 8.

[13] Chen L, Sun LM, Nagarajaiah S. Cable with discrete negative stiffness device and viscous damper: passive realization and general characteristics. *Smart Structures and Systems*, 2015; **15** (3): 627-643.

[14] Gazetas G. Formulas and Charts for Impedances of Surface and Embedded Foundations. *Journal of Geotechnical Engineering, ASCE*, 1991; **117** (9): 1363-1381.

[15] Smith MJ, Grigoriadis KM, Skelton RE. Optimal mix of passive and active control in structures. *Journal of Guidance, Control, and Dynamics*, 1992; **15** (4): 912-919.

[16] Soong TT. (1990). *Active Structural Control: Theory and Practice*, Longman Scientific &Technical, England.

[17] Yang J, Akbarpour A, Askar G. Effect of Time Delay on Control of Seismic-Excited Buildings. *Journal of Structural Engineering*, 1990; **116** (10): 2801-2814.

[18] Soong T, Reinhorn A, Wang Y, Lin R. Full-Scale Implementation of Active Control. I: Design and Simulation. *Journal of Structural Engineering*, 1991; **117** (11): 3516-3536.

[19] Reinhorn A, Soong T, Riley M, Lin R, Aizawa S, Higashino M. Full-Scale Implementation of Active Control. II: Installation and Performance. *Journal of Structural Engineering*, 1993; **119** (6): 1935-1960.

[20] Vanderplaats GN. (1984). *Numerical Optimization Techniques for Engineering Design*, McGraw-Hill Ryerson.

[21] Cheng FY, Jiang H, Lou K. (2008). "Chapter 9: Hybrid Control of Structures on Shallow Foundation with Existing and Generated Earthquakes." Smart Structures: Innovative Systems for Seismic Response Control, C. Press, ed., Taylor & Francis Group, LLC.

[22] Cimellaro GP. (2013). "Optimal Placement of controllers for seismic Structures." Design Optimization of Active and Passive Structural Control Systems, P. V. a. M. C. E. Lagaros N.D. , ed., IGI Global (formerly Idea Group Inc.), p. 1-33.

[23] Ohtori Y, Christenson RE, Spencer BF, Dyke SJ. Nonlinear Benchmark Control Problem for Seismically excited Buildings. *ASCE Journal of Engineering Mechanics*, 2004; **130** (4): 366-385.